NEW RESULTS FROM GAMMASPHERE*

F.S. STEPHENS

Nuclear Science Division, Lawrence Berkeley Laboratory
Berkeley, CA 94720, USA

(Received January 10, 1995)

The new gamma-ray detector array, Gammasphere, is described and compared with other new arrays. The physics from this detector system is discussed briefly and two topics are considered in greater detail. The first topic is "identical bands" where it is shown that the similarities between these bands are not accidental, but also that it is a phenomenon which is not yet understood. The second topic discusses the study of nuclear structure in neutron-rich nuclei formed in deep-inelastic reactions.

PACS numbers: 21.10. Re, 21.60. Ev, 23.20. Lv, 27.60. +j

1. Introduction

It is a pleasure to be here in Zakopane again, and I would like to thank the organizers for inviting me to give a talk on new results from Gammasphere. There is a lot happening now with the large new gamma-ray detector arrays and I will tell you first something about Gammasphere and how it compares with the other arrays, and then go on to some physics topics. I first thought to review all the physics highlights coming out of Gammasphere, but after contemplating a rather long list with two or three minutes per topic, I decided instead to pick two topics and discuss only these. The topics I chose are "Identical Bands" (an old favorite of mine) and "Nuclear Structure in Neutron Rich Nuclei".

2. Gammasphere and other arrays

Gammasphere is a 4π array that will consist of 110 Compton-suppressed germanium detectors. A photograph of one of the 110 detector modules

* Presented at the XXIX Zakopane School of Physics, Zakopane, Poland, September 5–14, 1994.

is shown in Fig. 1. The germanium detectors are approximately 7 cm in diameter and 8.5 cm in length and are in the endcap of the cryostat shown. The Compton suppressors are all of bismuth germanate (BGO) and there is a backplug behind the germanium detector (shown attached in Fig. 1), as well as a hexagonal shield around it (shown separately in Fig. 1). These are "standard" detectors, much like the ones in Eurogam I and GASP. I will discuss later an important modification we are now incorporating into the Ge detectors.

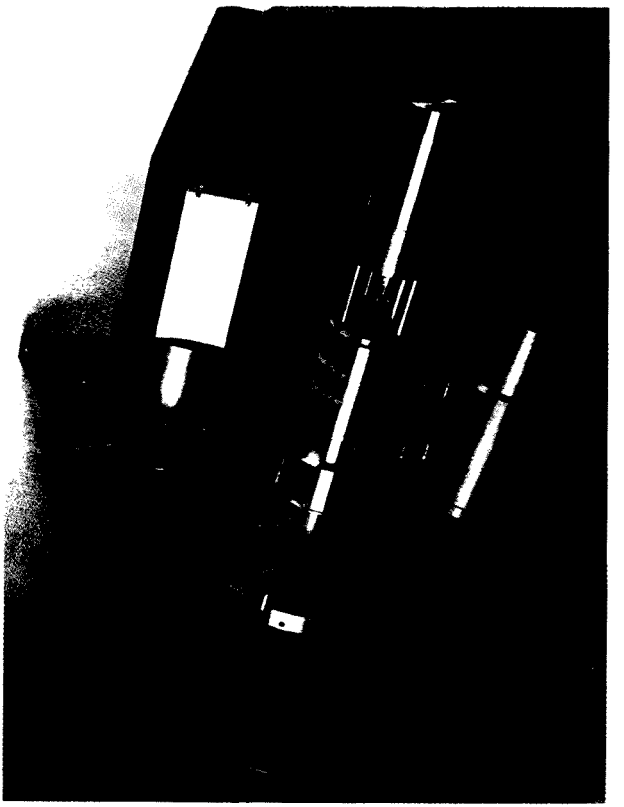

Fig. 1. Detector module components for Gammasphere.

Because the electronics and mechanical support stand for Gammasphere were not ready, operation began in an Early Implementation (EI) phase about one and one half years ago. This phase used 36 detectors, a temporary support stand, and the HERA electronics. A photograph of this arrangement is shown in Fig. 2. The detectors were located mostly forward and backward relative to the beam direction in order to minimize the effects of the Doppler broadening due to the finite opening angle of the Ge detectors. This phase of Gammasphere operated for almost a year and a half

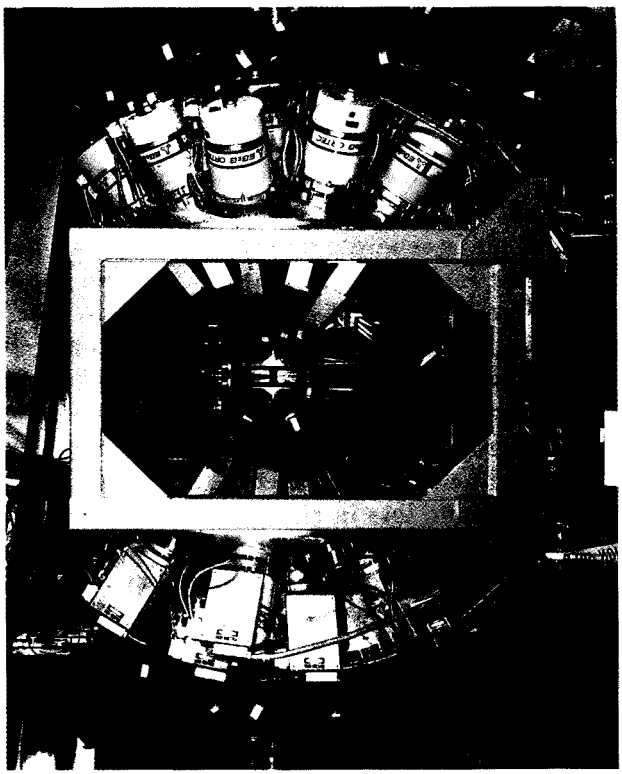

Fig. 2. Early Implementation arrangement for Gammasphere.

during which about 45 experiments utilized nearly 4000 hours of 88-Inch Cyclotron time. In this phase Gammasphere was about comparable in detection capabilities to Eurogam I and GASP (as discussed later). Currently this EI phase has been removed and the final stand and electronics for Gammasphere are being installed. Operation is expected to resume in November or early December with about 50 detectors. After that detectors will be received and put into operation at the rate of about one a week, resulting in the completion of Gammasphere with 110 detectors in October, 1995.

A major problem limiting the capabilities of these detector arrays for many types of experiment is the Doppler broadening of gamma-ray lines emitted from moving recoil nuclei due to the opening angle of the Ge detectors. In a typical fusion reaction, the product nucleus recoils forward with velocities of 3% of light. Since the Gammasphere detectors have opening angles of about 15°, a 1 MeV gamma ray emitted at 90° will have a width of 6.2 keV due to the Doppler effects, compared with the intrinsic line width

of these detectors of about 2 keV. Since the line width, or resolution, of the detectors is one of the most important factors determining the capability of the array, it is very important to reduce this broadening. There are several possible ways to approach this problem. We decided to keep the overall detector shape but divide it into two halves, each of which then subtends an angle only half as large as the original detector, thereby reducing the Doppler broadening effects by a factor of two. We first physically cut the Ge crystal in two and made separate detectors out of each half, which were then packaged together into a cryostat of the original shape ("sliced" in Fig. 3). This option resulted in an efficiency loss that was unacceptably large. As a second attempt we electrically divided the outer electrode of the crystal and read out a low resolution energy from each half ("segmented" in Fig. 3). The high resolution signal from the central electrode was unaffected. For 95incident gamma rays the crystal half with the most energy received the initial hit and could be Doppler corrected accordingly. These detectors were very successful, with no loss in efficiency or resolution compared with the original Gammasphere detectors. Approximately 70 or 80 of the 110 Gammasphere detectors will be of this segmented type. This improvement will about double the power of Gammasphere.

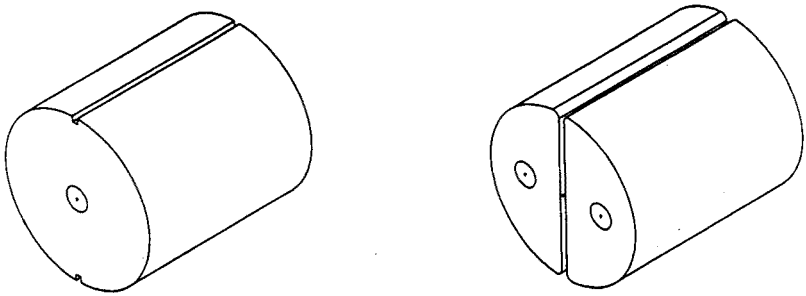

Fig. 3. Schematic illustrations of "Sliced" and "Segmented" Gammasphere Ge detectors.

The European arrays have also recognized the need for higher granularity to reduce the Doppler broadening. They have followed a somewhat different route to achieve this; employing clusters of smaller detectors rather than subdividing the existing ones. The "clovers", consisting of four smaller detectors, and the "clusters", of 7 tapered hexagonal detectors, are the ones so far developed. It is not so easy to compare these detector arrays. However, if we confine ourselves to the types of fusion reactions we have been discussing, then there are just three quantities that are important: the

energy resolution, the efficiency, and the spectral quality, *i.e.* the ratio of full-energy (peak) counts to total counts (P/T) ratio. There are several algorithms that combine these into a figure of merit, or "resolving power", but they are all rather similar. A plot of resolving power *vs.* calendar date, using one of these, is shown in Fig. 4. Differences of 20 or 30% are probably within the uncertainties, but the strong upward trend with time is impressive.

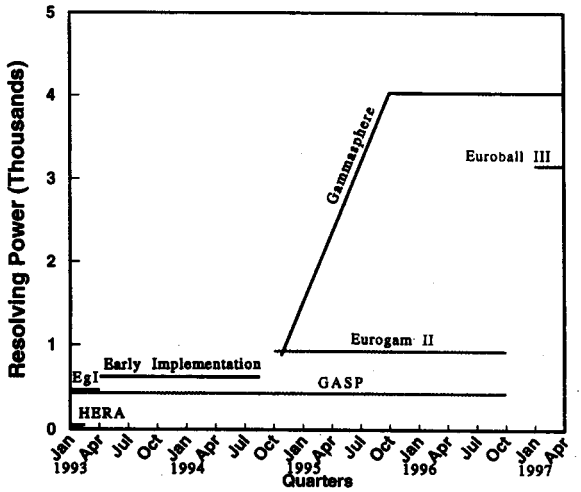

Fig. 4. Projected resolving powers for various detector systems as a function of date.

The first generation of arrays is represented in Fig. 4 by HERA and there were/are a number of others in that category, TESSA, 8π, Nordball, *etc.*, some of which are significantly better than HERA. The three second generation arrays, Eurogam I, GASP, and Gammasphere EI, have similar resolving powers, all about a factor of 10 better than the previous generation. That represented a very large improvement and much interesting physics has resulted. The third generation begins now with Eurogam II and Gammasphere, Phase I with 50–55 detectors. These are both about two times better than the second generation arrays. Gammasphere will improve as detectors are added and upon completion be another four times better in resolving power. Euroball III, with the first use of cluster detectors, will be comparable to the completed Gammasphere and both of these will be nearly 100 times better than the first generation of arrays. Although this discussion is for only one type of experiment (studies following heavy-ion fusion reactions) it gives an idea not only of the great increase in power of these arrays but also of their relationship to each other.

An enormous amount of physics has been studied using the second generation arrays. The following are a few examples of nuclear structure results from Gammasphere: at least 25 new superdeformed bands; the first Microball operation (SD bands in ^{81,83}Sr and ^{84}Zr); evidence for C4 symmetry in ^{194}Hg; studies of neutron-rich nuclei following DIC (Si strip detector); soft band termination in Sb and Te nuclei; identical bands (^{136}Nd); the first evidence for a superdeformed octupole band in ^{190}Hg; the first shape change in a SD band; the discovery of an $a = -1$ pseudospin band in ^{151}Dy; the first quadrupole moment of a SD excited band (*cf.* the yrast band); a band crossing in ^{192}Hg (Pairing?); the discovery of superdeformation in Bi and odd-mass Pb nuclei; unpaired spectroscopy beyond $I = 50$–^{156}Dy; and studies in $A = 140$ ($N = 80$) nuclei–^{142}Sm, ^{14x}Eu. Although I will only discuss two of these, I will be glad to try to answer questions you may have on some of the others. In addition to nuclear structure, experiments are being planned or discussed in other areas of physics. Some examples of these are: a precise determination of the Electro-Weak coupling constant; a test of QED (search for e^+e^- resonances); studies of neutron-rich nuclei from fission fragments and following deep inelastic collisions (DIC); nuclear reaction studies including DIC reaction mechanism and fusion dynamics; astrophysics, involving studies of *rp*-process nuclei and searches for strange matter; and finally the nuclear properties of the heaviest elements. I have listed these results and topics to illustrate that Gammasphere is already very productive and also that these arrays can and are being used to study a wide variety of physics.

3. Identical bands

Identical bands have been a hot topic in nuclear structure for several years now, and I want to describe some new analyses that Paul Fallon and I have made in this area. The present discussion will try to answer four questions. (1) What are identical bands? (2) Is this a statistically significant effect? (3) How identical are these bands? (4) How do they compare with what we expect? While answers to these questions are not fully available yet, we believe significant progress has been made.

Some basic properties of rotational bands are illustrated in Fig. 5. The rotational levels of a quantal system have energy spacings proportional to $I(I+1)$, where I is the angular momentum (spin) of the system. Rotational bands in nuclei have spins that increase progressively by either 1 or 2 units ($\hbar$) of angular momentum and for the latter case (illustrated in Fig. 5) the transitions between these levels are proportional to $(4I-2)$, or for spins large compared with 2 approximately to I. The difference in energy between transitions is then independent of I, so that the spectrum of gamma rays

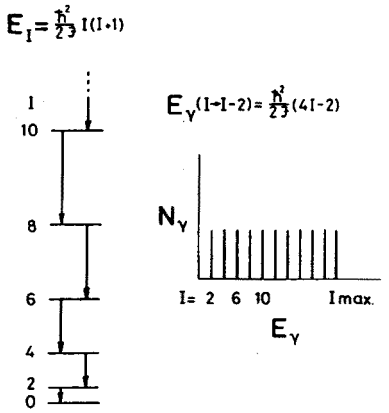

Fig. 5. Energy levels and schematic (E2) gamma-ray spectrum of a quantal rotor.

looks like a picket fence, as illustrated at the right of Fig. 5. This is a very characteristic pattern and makes it easy to identify weakly populated rotational bands.

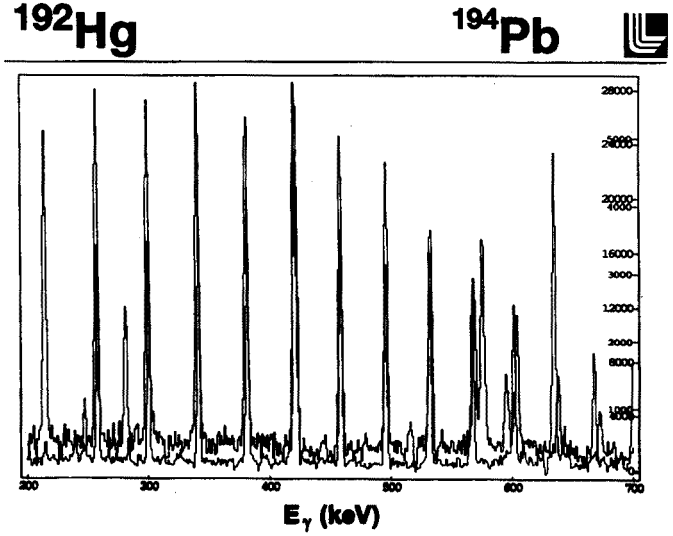

Fig. 6. Superposed sections of gamma-ray spectra from ^{192}Hg and ^{194}Pb.

Sections of the gamma-ray spectra from a rotational band in each of two different superdeformed nuclei are shown in Fig. 6. It is easy to recognize the picket fence character described above, although the separations between the transitions becomes significantly smaller at the top of the bands. The astounding feature is the virtually identical gamma-ray energies over a span of about 10 transitions ($20\hbar$). This feature was first discovered in the mass-

150 region of superdeformed nuclei [1], but is probably even more prevalent in this mass-190 region [2]. There are two aspects to notice here: first, the equal separation between the gamma-ray energies implies that the ($J(2)$) moments of inertia are the same for the two nuclei; and second, the fact that the peaks lie on top of each other implies more and this can be expressed by saying that the alignments are quantized. This is the phenomenon of "identical bands".

It is important to decide first if this similarity is accidental or not. An argument has been made that with 40–50 known bands in this region there are about 2000 pairs of bands and some of these will accidentally be very similar. Perhaps the two bands in Fig. 6 are just one of these accidental pairs. This is one of the questions Paul and I set out to answer. To be impartial, we decided to compare every band with every other band in a given region, and within a band to compare each transition with the one closest in energy in the other band. This raises an important point — the spins are not measured and integer values may be added or subtracted without contradicting anything known. Thus there is only a range of $1\hbar$ that is significant and we can always add or subtract the energy equivalent to $1\hbar$ to bring the transition energy difference into the chosen range. The energy equivalent of $1\hbar$ is easy to evaluate since the energy difference between two adjacent transitions in the same band corresponds to exactly $2\hbar$.

In this way, a comparison of all the bands in the 190-, 150, and 130-mass regions is shown in Fig. 7, which plots the number of pairs of transitions as a function of the energy difference between the transitions of the pair. The energy regions corresponding to the chosen $1\hbar$ ranges are indicated by the solid dots and the open dots are just repetitions to put the $1\hbar$ region into some context. It is apparent from Fig. 7 that while there is no general structure in the mass 150 or 130 regions, but there is a strong preference centered around zero for the energy difference between pairs in the mass 190 region. Thus the occurrence of similar bands is not purely accidental, at least in the mass-190 region. In fact, the random (flat in Fig. 7) distribution of energy differences in the other regions does not exclude "identical" bands in those regions, but simply shows their number is too small to see in these global comparisons.

To learn more one can restrict the comparison. In Fig. 8 some restricted comparisons within the mass–190 region are shown. The first, Fig. 8a, compares only bands in nuclei of the same element, *i.e.* having the same Z. In other words Fig. 8a looks at the effect of changing only the number of neutrons. It is sensitive to the properties of the neutron orbitals in the nuclei, and shows that the tendency to be identical is considerably stronger when only neutrons are changed (Fig. 8a) than when neutrons and/or protons are changed (Fig. 7a). The complementary distribution, where only protons

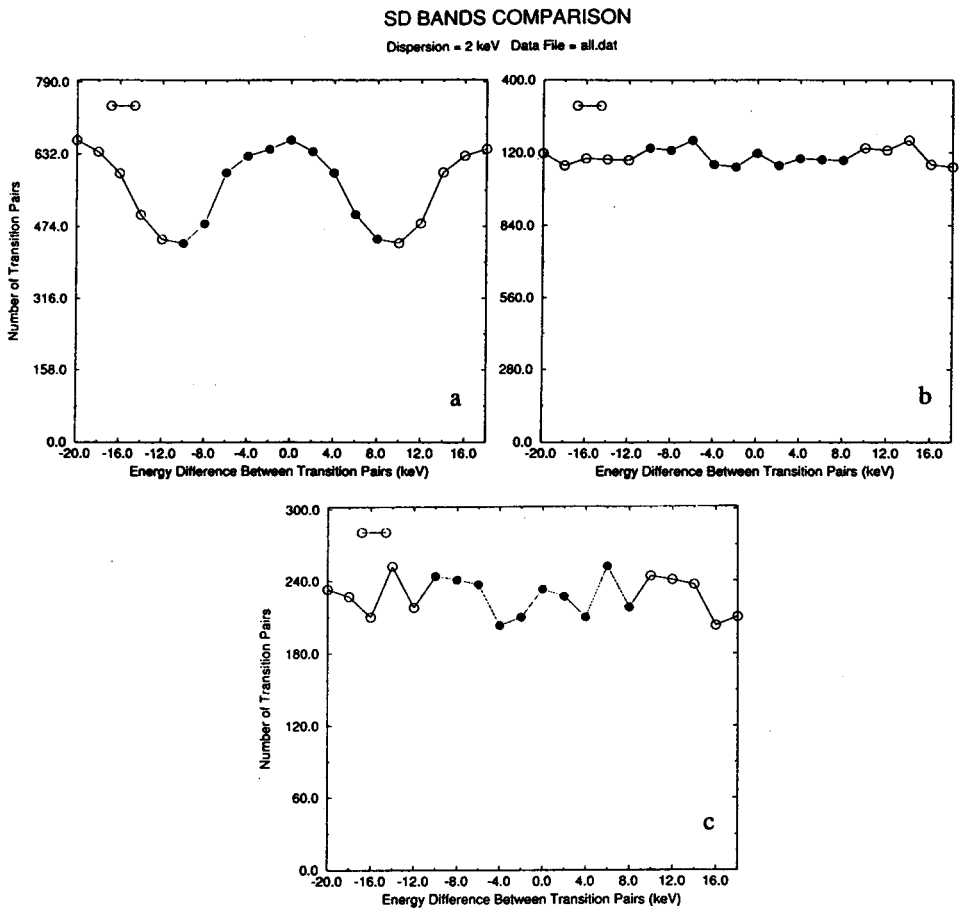

Fig. 7. Distribution of energy differences between pairs of transitions in superdeformed bands of the mass: a — 190 (parameters used: Z-range: 80–82, Z-difference: 0–20, N-range: 110–120, N-difference: 0–20, max. nucleon difference: 20, transition energy range: 200); b — 150 (parameters used: Z-range: 64–66, Z-difference: 0–20, N-range: 80–87, N-difference: 0–20, max. nucleon difference: 20, transition energy range: 400–2000); and c — 130 (parameters used: Z-range: 57–60, Z-difference: 0–20, N-range: 73–77, N-difference: 0–4, max. nucleon difference: 20, transition energy range: 700–1000) regions.

are allowed to change is shown in Fig. 8b. This distribution is also far from random, however, the variation in energy difference is wider than for the neutrons and the center of the distribution is clearly not at zero. These are properties we need to understand from the proton orbitals that are changing in going from nucleus to nucleus. I will come back to consider how we try to relate some of these distributions to the calculated properties of the orbitals

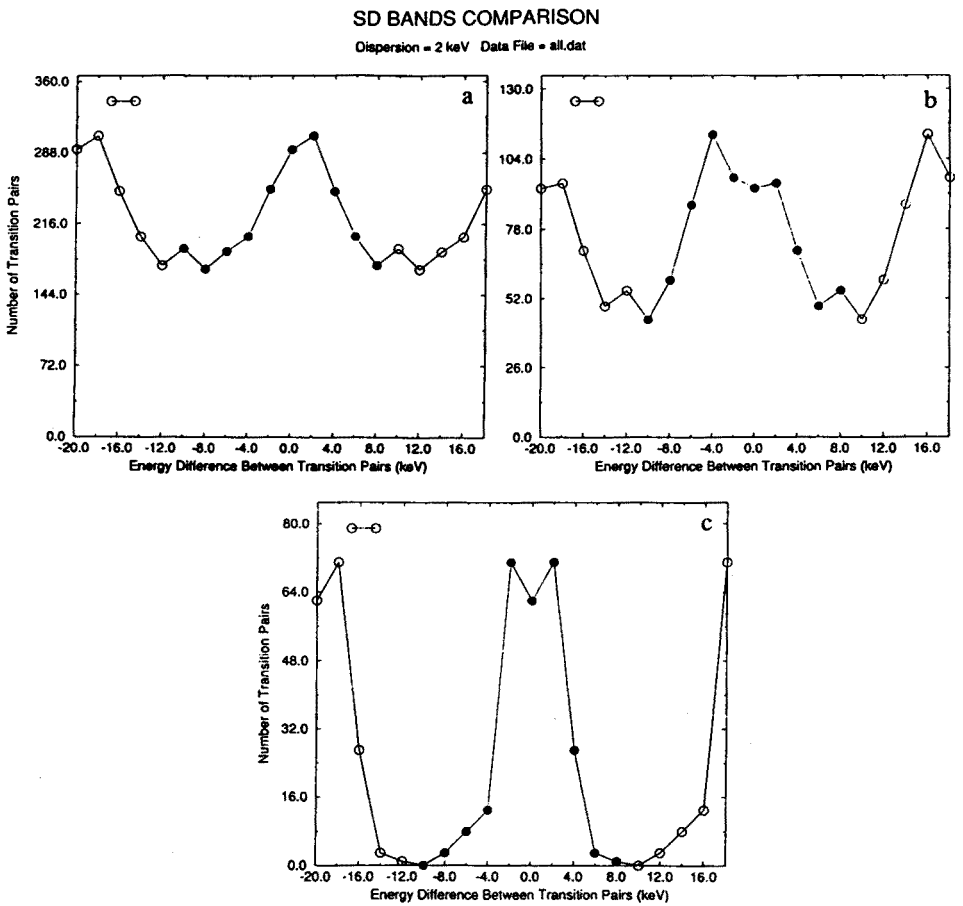

Fig. 8. Restricted comparisons of energy differences between pairs of transitions in superdeformed bands of the mass 190 region: a — no change in Z; (parameters used: Z-range: 80–82, Z-difference: 0–0, N-range: 110–120, N-difference: 0–20, max. nucleon difference: 20, transition energy range: 200–1000); b — no change in N (parameters used: Z-range: 80–82, Z-difference: 0–20, N-range: 110–120, N-difference: 0–0, max. nucleon difference: 20, transition energy range: 200–1000); and c — "known" identical bands in $^{191-194}$Hg (parameters used: Z-range: 80–80, Z-difference: 0–0, N-range: 110–120, N-difference: 0–20, max. nucleon difference: 20, transition energy range: 200–1000).

A final restriction of the data compared is shown in Fig. 8c. Here we have picked out one set of the "known" identical bands in this mass region. They are bands in ^{191}Hg, ^{192}Hg, ^{193}Hg, and ^{194}Hg and, as expected, the distribution has a very pronounced structure. What we are interested in here is the width of this distribution, which relates to the question: how

identical is "identical". The width (FWHM) is about 1/3 $\hbar$, and over the range of one 1$\hbar$, the bands are not so precisely identical, however, for a band that continues with this precision for 10 transitions or 20$\hbar$ (which many do), this becomes quite impressive. It is now interesting to look at what current calculations give for this width.

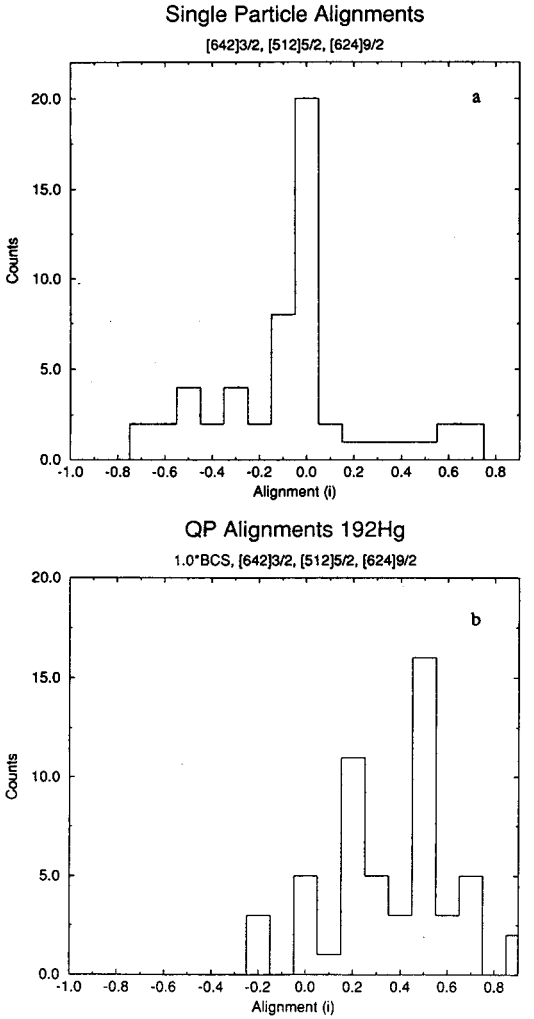

Fig. 9. Calculated energy differences between pairs of transitions for the indicated orbitals in superdeformed nuclei of the mass 190 region: a — without, and b — with inclusion of pairing.

The neutron orbits probably responsible for the selected "identical" bands in Fig. 8c are: [642]3/2; [512]5/2; and [624]9/2. Using results from the cranked Woods-Saxon potential (not including pairing) we can calculate the effect on the energy difference between transition pairs for bands with and without one of these orbits occupied. The calculated results are treated exactly like the experimental data and a plot equivalent to that in Fig. 8c is shown in Fig. 9a. Of course, we do know the calculated spins and those are included in Fig. 9a, so that zero is really zero and not any other integer. We have used alignment for the abscissa scale rather than energy, but the transformation, as mentioned, is just $2\hbar$ is equal to the difference in energy between adjacent transitions in one of the bands. This amounts to about 20 keV per $\hbar$ in the mass 190 region, so that the range for the abscissa in Fig. 9 is very nearly equivalent to that for Figs 7 and 8. The surprising result is that the calculated bands are even more "identical" than the experimental ones. However, remember that the moments of inertia are assumed to be equal and there is no pairing in the calculation. The effect of simple monopole pairing on this orbital alignment can be calculated and is shown in Fig. 9b. It is apparent that the identicality of the bands is lost, even though the moments of inertia are still assumed to be equal. The result here is that the particular orbital contributions to the spin (alignment) are consistent with the data until pairing effects are included. Obviously we do not yet understand the pairing effects in these nuclei.

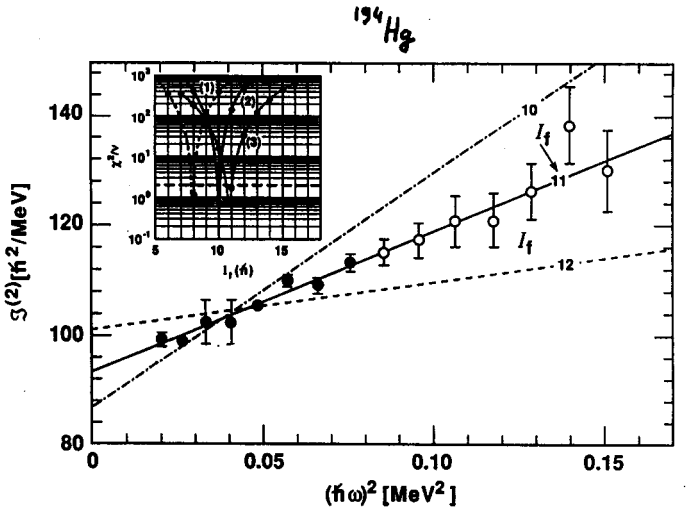

Fig. 10. Illustration of the spin determination for a band in ^{194}Hg from the plot of moment of inertia *vs.* rotational frequency squared. The inset shows the χ^2 per degree of freedom plots for all three known bands in ^{194}Hg, each of which indicates a nearly exactly integer spin.

In the above discussion we have accepted the position that the spins are not experimentally determined. However, a method has been put forward [3] for determining the spins in the mass-190 region, and while it is model dependent, there are some compelling reasons to believe it gives the correct spins. The method is illustrated in Fig. 10, where the $J^{(2)}$ moment of inertia ($J^{(2)}$ is $4/\Delta E_\gamma$, where ΔE_γ is the energy difference between adjacent transition energies) is plotted against the square of the frequency (the frequency is half the gamma-ray energy). The points are approximately linear, and we can extrapolate them to zero frequency and integrate back up to get the spin at any frequency. A test of the method is that the spin in this even mass nucleus has to be integer and the χ^2 plot in the inset of Fig. 10 shows that the spin determined for this band (3) is indeed very close to an integer — $11\hbar$. The other two bands (1 and 2) in ^{194}Hg are also very close to integers. This is a rather strong indication that the spins are correct.

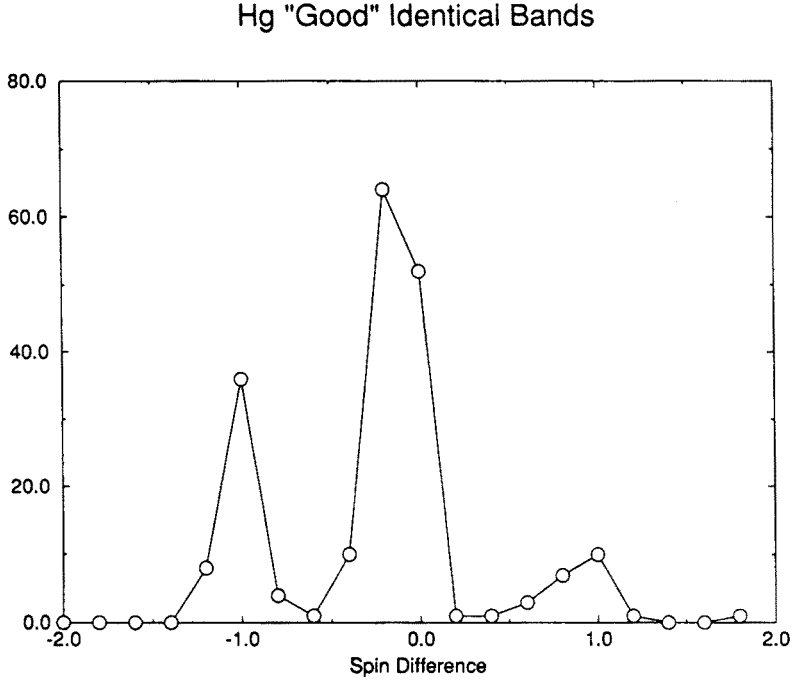

Fig. 11. Data of Fig. 8c using spins determined with the method illustrated in Fig. 10.

If we use the spins determined by this method, the plot in Fig. 8c for the "known" identical bands becomes that shown in Fig. 11, where we have converted the units of the abscissa from energy to spin (equivalent to alignment for the calculations) and lengthened the range. There is no

longer any limitation in the range of the data, although positive and negative values are equivalent, as they just reflect the order in which the bands are compared. The peaks at 1 and -1 (which are equivalent) are clear and do not appear in the calculations at all. This is something quite unexpected and appears to be either a peculiar pairing effect on the moments of inertia or some new alignment effect.

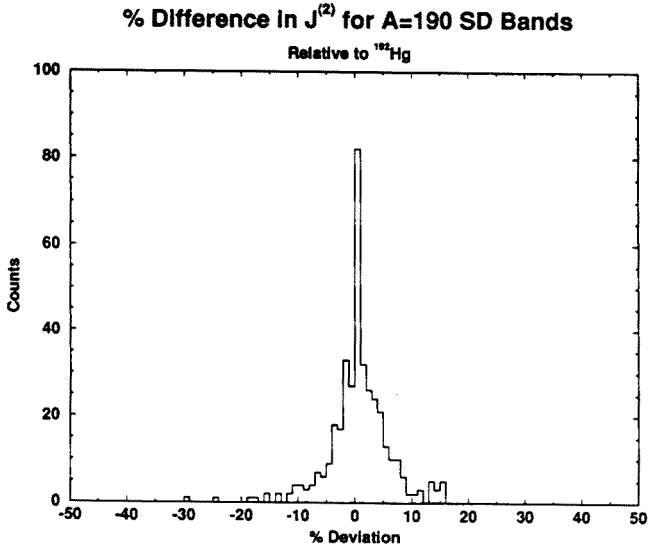

Fig. 12. Distribution of moments of inertia for superdeformed bands in the mass 190 region compared with that of ^{192}Hg.

In the above we have assumed the bands have the same moment of inertia and it is interesting to examine this assumption for a moment. Fig. 12 shows the moments of inertia for the bands in the mass 190 region compared to that of ^{192}Hg. There is first a sharp peak, within about 1% of that of ^{192}Hg and also a broader peak that extends to about $\pm 5\%$. The latter is something like we would expect based on calculations of blocking effects in the pairing for odd-mass nuclei. However, the sharp peak is not understood, and again tells us there is something wrong with our concept of pairing in these nuclei. It seems clear that these identical bands have a lot to teach us about the behavior of nuclei.

4. Nuclear structure in neutron–rich nuclei

Nuclear fusion reactions with stable targets and beams cannot make neutron-rich nuclei, and, even using radioactive-ion beams will have difficulty getting beyond the stable nuclei. Fortunately there are several other

ways to produce these nuclei for nuclear structure studies. So far one of the principal ways has been the study of fission products, which are generally very neutron rich. However, a limitation of this method is that one cannot control which nuclei are produced — fission products are distributed over a region, albeit rather broad, around one-half the parent nuclear mass. Also the angular momentum input is fixed and centered around approximately $10\hbar$. A second method to produce neutron-rich nuclei is by transferring neutrons into the heaviest stable nuclei, and for multiple neutron transfers and reasonably large cross sections, this means deep inelastic collisions (DIC). This method also has the advantage that it can bring in larger amounts of angular momentum. A number of nuclear structure studies using the DIC method have been made [4–6] and the Krakow group has pioneered this direction. There is a paper later in this meeting by Fornal on this topic. However, so far all the DIC structure studies have used a thick backing to stop the recoiling products in about 1 psec, so that the highest energy (and spin) states that have lifetimes shorter than this are smeared out in the spectrum. I am going to report some work, led by I. Y. Lee, that removes this limitation and thereby studies the highest spins produced in these reactions.

We studied the reaction, ^{176}Yb + ^{48}Ca at 250 MeV, and measured the energy and angle of the Ca-like fragment in a silicon strip detector. From these quantities we could select the DIC reactions and also correct the gamma rays emitted for Doppler effects due to the velocity of the (either) recoiling fragment. The annular Si detector was 300 microns thick and had an inner diameter of 4.8 cm, an outer diameter of 9.6 cm and an active area of 53 cm^2. There were 16 concentric rings to determine the scattering angle and also 16 sectors to determine the azimuthal angle. This detector worked very well, both to select DIC products (by the Ca-like fragment energy) and to provide adequate Doppler corrections.

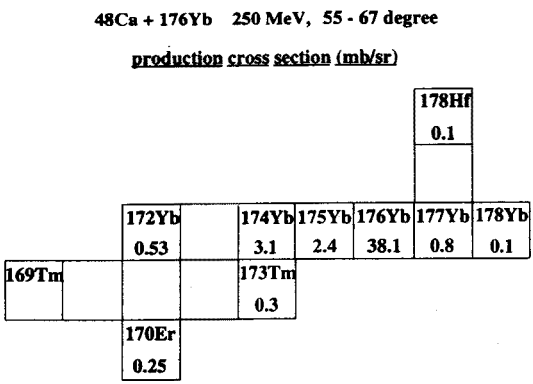

Fig. 13. Cross sections for producing some isotopes of Hf, Yb, Tm, and Er from DIC reactions of ^{48}Ca on ^{176}Yb.

The Yb-like products identified are shown in Fig. 13 relative to the position of the target, ^{176}Yb. This is not a complete profile because lines are not known in some of the products while others are obscured by stronger lines in other products. Because the projectile was neutron poorer than the target, the flow of neutrons was stronger out of the heavy fragment than into it. Thus ^{174}Yb was stronger than ^{178}Yb, though the latter could be studied. Coulomb effects, however, caused protons also to transfer preferentially out of the heavy fragment and this produced very neutron-rich Tm isotopes (many of the Er lines were masked). Overall we were very pleased with these yields and expect improvement in the yields of neutron-richer products when heavier (neutron richer) projectile nuclei are used.

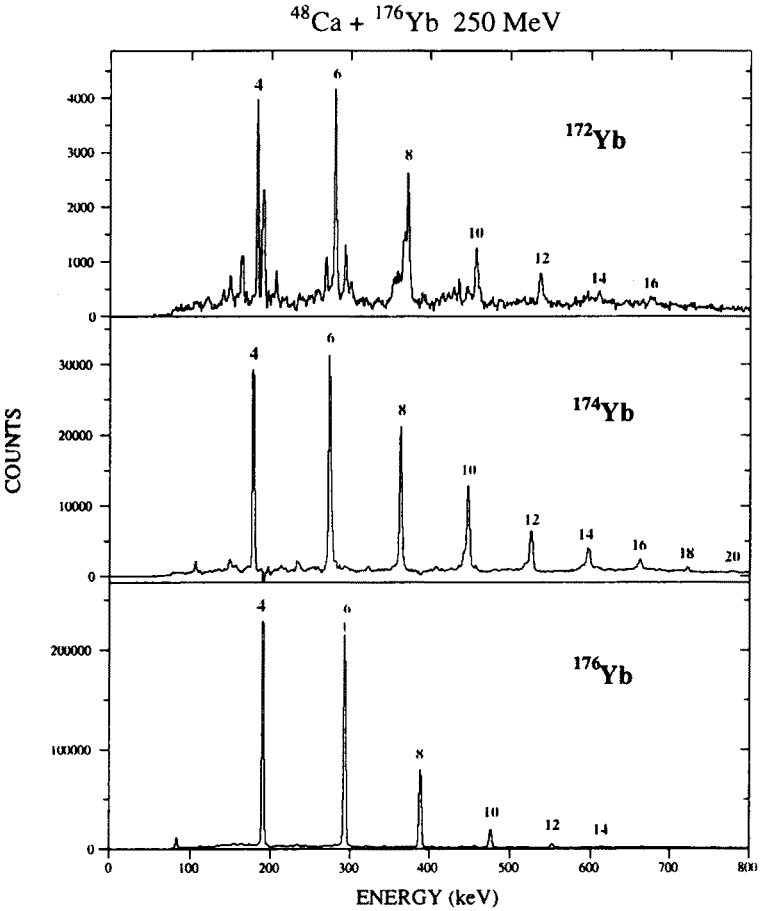

Fig. 14. Coincidence spectra of gamma rays from ^{172,4,6}Yb produced in the DIC reaction of Fig. 13.

Gamma-ray spectra from ^{176}Yb and the lighter even-even Yb isotopes are shown in Fig. 14 and that obtained for ^{178}Yb is shown in Fig. 15. The level schemes for ^{177}Yb and ^{178}Yb derived from this work are shown in Fig. 16, where, in both cases, only the first three levels were previously known. It is clear that a lot of new spectroscopic data will come from this first attempt to study these reactions using Gammasphere, however the main point here is to show that the DIC method can be extended to study the fast high-spin transitions.

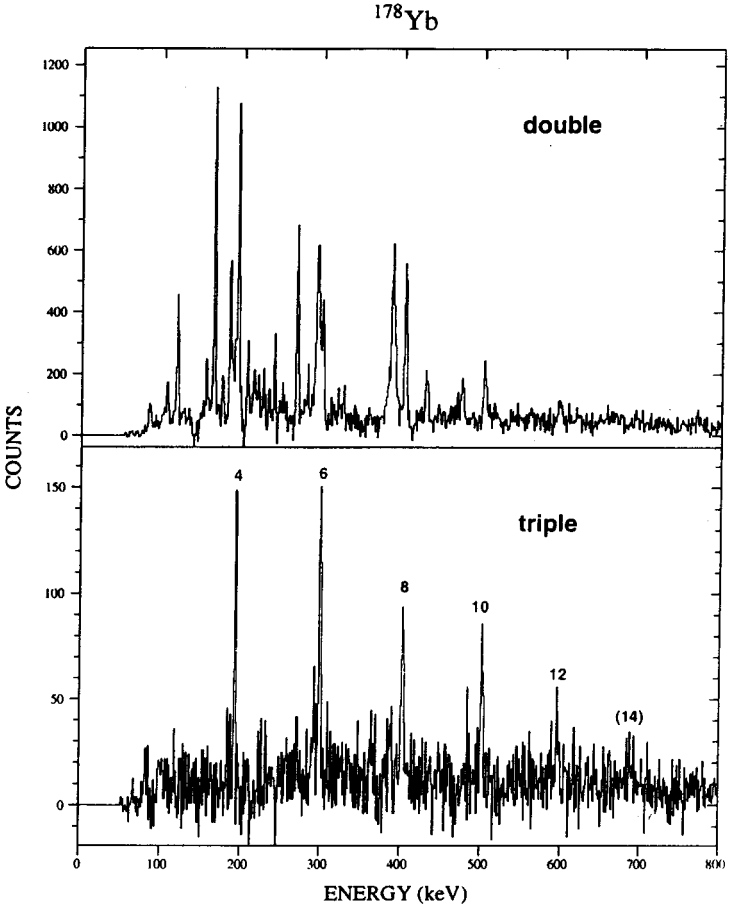

Fig. 15. Double and triple coincidence spectra of gamma rays from ^{178}Yb produced as in Fig. 14.

To conclude this discussion of the DIC method of producing neutron-rich nuclei, it is interesting to note that ^{178}Yb cannot be made in a typical heavy-ion fusion reaction even if one had a radioactive beam (or target) of

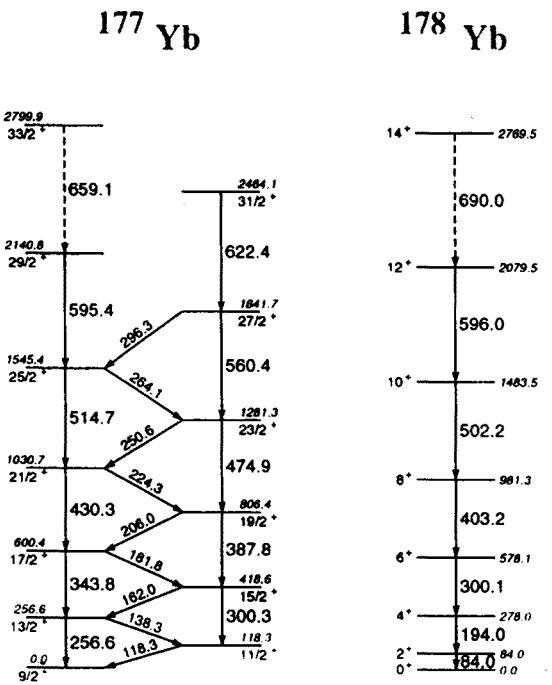

Fig. 16. Level schemes constructed from the DIC data for ^{177,8}Yb, where only the first three levels of each nucleus were previously known.

^{132}Sn and that is not likely in the near future. In addition, there is a very good possibility of making ^{180}Yb, or even heavier isotopes, using heavier stable projectiles in the DIC method — ^{208}Pb or ^{176}Yb, itself, would be very interesting projectiles to use. It seems clear that these reactions will provide a powerful and general method to study the structure of neutron-rich nuclei.

The work described here has been done largely by the Nuclear Structure groups at the Lawrence Berkeley Laboratory and the Lawrence Livermore National Laboratory. This work has been supported in part by the Director, Office of Energy Research, Division of Nuclear Physics of the Office of High Energy and Nuclear Physics of the U. S. Department of Energy under Contract Nos. DE-AC03-76SF00098 (LBL) and W-7405-ENG-48 (LLNL).

REFERENCES

[1] T. Byrski *et al.*, *Phys. Rev. Lett.* **64**, 1650 (1990).
[2] F.S. Stephens *et al.*, *Phys. Rev. Lett.* **64**, 2623 (1990).

[3] J.A. Becker *et al.*, *Phys. Rev.* **C41**, 9 (1990).
[4] K. Rykaczewski *et al.*, *Nucl. Phys.* **A499**, 529 (1989).
[5] H. Tokai *et al.*, *Phys. Rev.* **C38**, 1247 (1988).
[6] R. Broda *et al.*, *Phys. Rev. Lett.* **68**, 1671 (1992).